

# Spinor Field at the Phase Transition Point of Reissner-Nordström de Sitter Space

Yan Lyu · Li-Qing Zhang · Wei Zheng · Qing-Chao Pan

Received: 9 February 2010 / Accepted: 13 April 2010 / Published online: 27 April 2010  
© Springer Science+Business Media, LLC 2010

**Abstract** The radial parts of Dirac equation between the outer black hole horizon and the cosmological horizon are solved in Reissner-Nordström de Sitter (RNds) space when it is at the phase transition point. We use an accurate polynomial approximation to approximate the modified tortoise coordinate  $\hat{r}_*$  in order to get the inverse function  $r = r(\hat{r}_*)$  and the potential  $V(\hat{r}_*)$ . Then we use a quantum mechanical method to solve the wave equation numerically. We consider two cases, one is when the two horizons are lying close to each other, the other is when the two horizons are widely separated.

**Keywords** Dirac equation · The phase transition point · Reissner-Nordström de Sitter space

## 1 Introduction

Since Chandrasekhar separated the Dirac equation in Kerr geometry into radial and angular parts [1], a considerable amount of work relating to Dirac fields around black holes has been carried out in the literature [2–9]. In recent years, Chakrabarti and Mukhopadhyay studied the behavior of Dirac particles around Schwarzschild and Kerr black hole by WKB approximation method and quantum mechanical method respectively [10–13]. They solved the spatially complete radial equation successfully, but they didn't consider the black hole with cosmological horizon. So in [14–17], we extended their work to Schwarzschild-de Sitter (SdS) space and the quasi-extreme RNds space. Different from their work, we used tangent, logarithm and polynomial approximation respectively to approximate the modified tortoise coordinate in order to solve the Dirac equation in the region between the black hole horizon and the cosmological horizon. We found the polynomial approximation is more accurate. So in this present paper, we will discuss Dirac field at the phase transition point of RNds geometry by using the polynomial approximation.

Y. Lyu (✉) · L.-Q. Zhang · W. Zheng · Q.-C. Pan

College of Physics Science and Technology, Shenyang Normal University, Shenyang 110034, Liaoning Province, People's Republic of China  
e-mail: yanlvthp@yahoo.com.cn

The Reissner-Nordström (RN) black hole is in fact a charged Schwarzschild black hole. When a positive cosmological constant  $\Lambda$  is taken into account, the RN space turns to be the RNdS space. Thus the space is bounded by three horizons, an inner horizon  $r_{e-}$  and an outer one  $r_{e+}$  of RN black hole, and a cosmological horizon  $r_c$ , which is determined by the value of the cosmological constant  $\Lambda$ . The region of physical significance is the bulk between the latter two horizons. There are two limiting cases of our special interest. The first one is the two horizons are very close to each other. The second one is the two horizons are far apart. Our main motivation is to give the variation of the Dirac waves in the whole range when the black hole is at the phase transition point.

Throughout the paper, the signature  $(- +++)$  is adopted, and  $\hbar$ ,  $c$  and  $G$  (Newtonian gravitational constant) are all taken as unity.

## 2 The Wave Equation

For a spherically symmetric system the line element takes the form

$$ds^2 = -f(r)dt^2 + \frac{1}{f(r)}dr^2 + r^2d\theta^2 + r^2\sin^2\theta d\varphi^2. \quad (1)$$

In our case

$$f(r) = 1 - \frac{2M}{r} + \frac{Q^2}{r^2} - \frac{1}{3}\Lambda r^2, \quad (2)$$

where  $M$  is the mass of the black hole,  $Q$  is the charge of the black hole.

Following Chandrasekhar [1], we separate Dirac equation in RNdS geometry into radial and angular equations. The equations governing the radial wave-functions  $R_{\pm 1/2}$  corresponding to spin  $\pm \frac{1}{2}$ , respectively, are given by

$$\Delta^{1/2}\mathcal{D}_0R_{-1/2} = (\lambda + imr)\Delta^{1/2}R_{+1/2}; \quad \Delta^{1/2}\mathcal{D}_0^\dagger\Delta^{1/2}R_{+1/2} = (\lambda - imr)R_{-1/2}, \quad (3)$$

where the operators  $\mathcal{D}_n$  and  $\mathcal{D}_n^\dagger$  are given by

$$\mathcal{D}_n = \partial_r + \frac{ir^2\sigma}{\Delta} + 2n\frac{r - M - \frac{2}{3}\Lambda r^3}{\Delta}; \quad \mathcal{D}_n^\dagger = \partial_r - \frac{ir^2\sigma}{\Delta} + 2n\frac{r - M - \frac{2}{3}\Lambda r^3}{\Delta}, \quad (4)$$

and

$$\Delta \equiv r^2 - 2Mr + Q^2 - \frac{\Lambda}{3}r^4. \quad (5)$$

In the above formulas  $n$  is an integer or half-integer,  $\sigma$  is the frequency of the incident wave,  $m$  is the rest mass of the Dirac particle and  $\lambda$  is the eigenvalue of the Dirac equation.  $\Delta$  is called horizon function.

The equations governing the angular wave-functions  $S_{\pm 1/2}$  corresponding to spin  $\pm \frac{1}{2}$ , respectively, are given by

$$L_{1/2}S_{+1/2} = -\lambda S_{-1/2}; \quad L_{1/2}^\dagger S_{-1/2} = \lambda S_{+1/2}, \quad (6)$$

where the operators  $L_n$  and  $L_n^\dagger$  are given by

$$L_n = \partial_\theta + n \cot\theta + m \operatorname{cosec}\theta, \quad L_n^\dagger = \partial_\theta + n \cot\theta - m \operatorname{cosec}\theta. \quad (7)$$

The cosmological constant  $\Lambda$  and the charge  $Q$  are all included in the horizon function  $\Delta$ , they only affect the radial parts of Dirac equation. The angular equations have the same form with that in Schwarzschild geometry. The eigenvalue of the angular equation for spin  $\pm\frac{1}{2}$  is obtained as  $\lambda^2 = (l + 1/2)^2$  [7, 18, 19], where  $l$  is the orbital quantum number. Here, we choose  $l = \frac{1}{2}$ , which appears to have greater interest [7], and  $\lambda = 1$ .

The radial equations (3) are in coupled form. Next we will decouple them by Chandrasekhar's approach.

We define tortoise coordinate

$$r_* = \int \frac{dr}{f(r)}. \quad (8)$$

In our case,  $f(r) = \frac{\Delta}{3r^2}(r - r_o)(r - r_{e+})(r - r_{e-})(r_c - r)$ , where  $r_o = -(r_{e-} + r_{e+} + r_c)$ , which is of no physical significance. Also define surface gravities  $\kappa_i$ ,

$$\kappa_i = \frac{1}{2} \left| \frac{df}{dr} \right|_{r=r_i}. \quad (9)$$

Then the tortoise coordinate in RNdS space takes the form

$$r_* = \frac{1}{2\kappa_{e+}} \ln \left| \frac{r}{r_{e+}} - 1 \right| - \frac{1}{2\kappa_{e-}} \ln \left| \frac{r}{r_{e-}} - 1 \right| - \frac{1}{2\kappa_c} \ln \left| \frac{r}{r_c} - 1 \right| + \frac{1}{2\kappa_o} \ln \left| \frac{r}{r_o} - 1 \right|. \quad (10)$$

In terms of  $r_*$ , the operators  $\mathcal{D}_0$  and  $\mathcal{D}_0^\dagger$  take the forms

$$\mathcal{D}_0 = \frac{r^2}{\Delta} \left( \frac{d}{dr_*} + i\sigma \right), \quad \mathcal{D}_0^\dagger = \frac{r^2}{\Delta} \left( \frac{d}{dr_*} - i\sigma \right). \quad (11)$$

Choosing  $\Delta^{1/2} R_{+1/2} = P_{+1/2}$ ,  $R_{-1/2} = P_{-1/2}$ , (3) becomes

$$\left( \frac{d}{dr_*} + i\sigma \right) P_{-1/2} = \frac{\Delta^{1/2}}{r^2} (1 + imr) P_{+1/2}, \quad \left( \frac{d}{dr_*} - i\sigma \right) P_{+1/2} = \frac{\Delta^{1/2}}{r^2} (1 - imr) P_{-1/2}. \quad (12)$$

Now we define a new variable  $\theta = \tan^{-1}(mr)$ , which gives

$$(1 \pm imr) = e^{\pm i\theta} \sqrt{1 + m^2 r^2}. \quad (13)$$

Also define

$$P_{+1/2} = \psi_{+1/2} \exp \left[ -\frac{1}{2} i \tan^{-1}(mr) \right]; \quad P_{-1/2} = \psi_{-1/2} \exp \left[ +\frac{1}{2} i \tan^{-1}(mr) \right], \quad (14)$$

and further choosing  $\hat{r}_* = r_* + \frac{1}{2\sigma} \tan^{-1}(mr)$  so that  $d\hat{r}_* = (1 + \frac{\Delta}{r^2} \frac{m}{2\sigma} \frac{1}{1+m^2r^2}) dr_*$ , and  $Z_\pm = \psi_{+1/2} \pm \psi_{-1/2}$ , the above equations become

$$\left( \frac{d}{d\hat{r}_*} - W \right) Z_+ = i\sigma Z_-; \quad \left( \frac{d}{d\hat{r}_*} + W \right) Z_- = i\sigma Z_+, \quad (15)$$

where

$$W = \frac{\Delta^{1/2} (1 + m^2 r^2)^{3/2}}{r^2 (1 + m^2 r^2) + m \Delta / 2\sigma}. \quad (16)$$

From these equations, we readily obtain a pair of independent one-dimensional wave equations

$$\left( \frac{d^2}{d\hat{r}_*^2} + \sigma^2 \right) Z_{\pm} = V_{\pm} Z_{\pm}, \quad (17)$$

where

$$\begin{aligned} V_{\pm} &= W^2 \pm \frac{dW}{d\hat{r}_*} \\ &= \frac{\Delta^{1/2}(1+m^2r^2)^{3/2}}{[r^2(1+m^2r^2)+m\Delta/2\sigma]^2} \\ &\times \left\{ \Delta^{1/2}(1+m^2r^2)^{3/2} \pm \left[ \left( r - M - \frac{2}{3}\Lambda r^3 \right)(1+m^2r^2) + 3m^2r\Delta \right] \right\} \\ &\mp \frac{\Delta^{3/2}(1+m^2r^2)^{5/2}}{[r^2(1+m^2r^2)+m\Delta/2\sigma]^3} \left[ 2r(1+m^2r^2) + m \left( r - M - \frac{2}{3}\Lambda r^3 \right) \right] / \sigma + 2m^2r^3. \end{aligned} \quad (18)$$

### 3 About the Parameters

In follow calculations, we choose the parameters in such a way [10] that there is a significant interaction between the particle and the black hole, then the Compton wavelength of the incoming wave is of the same order as RNdS radius. Similarly, the frequency of the incoming particle will be of the same order as inverse of time. So  $m \sim \sigma$ , we choose  $m = \sigma = 0.8$ . When the charge of the black hole  $Q$  is taken as a constant the thermal capacity of the RN black hole is given as [20]

$$C_Q = \left( \frac{\partial M}{\partial T} \right)_Q = 2\pi r_{e+}^2 \frac{(M^2 - Q^2)^{1/2}}{M - 2(M^2 - Q^2)^{1/2}}. \quad (19)$$

It is easily seen that  $C_Q < 0$  when  $Q^2 < \frac{3}{4}M^2$  while  $C_Q > 0$  when  $Q^2 > \frac{3}{4}M^2$ . Thus  $Q^2 = \frac{3}{4}M^2$  can be taken as the phase transition point of RN space, and the mass of the black hole  $M$  is set to be unity hereafter, thus  $Q^2 = \frac{3}{4}$ .

As mentioned above, we consider two cases. It is found that there is an upper limit of  $\Lambda (= 0.1547)$  to ensure (2) have four real roots when the cosmological horizon is very close to the outer horizon of the black hole. The four roots are  $r_{e-} = 0.4969$ ,  $r_{e+} = 2.3633$ ,  $r_c = 2.3688$  and  $r_o = -5.2289$ . The cosmological constant  $\Lambda \ll 1$  when the two horizons are widely separate, and it can be taken as  $\Lambda = 0.001$ , then  $r_{e-} = 0.5000$ ,  $r_{e+} = 1.5017$ ,  $r_c = 53.7508$  and  $r_o = -55.7525$ .

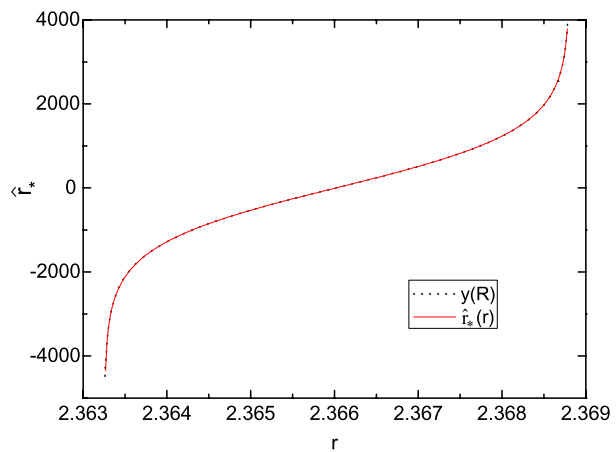
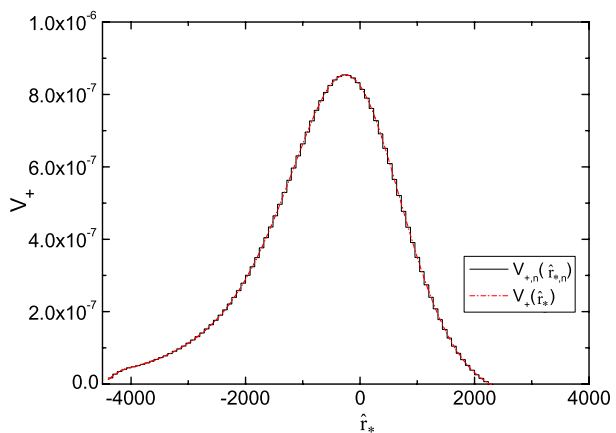
### 4 Solution of the Wave Equation

To solve (17), we need  $V(\hat{r}_*)$ . Equation (18) for  $V(r)$  thus must be inverted. Here we introduce the polynomial approximation  $R = R(y)$  to get the inverse function of modified tortoise coordinate  $\hat{r}_* = \hat{r}_*(r)$  and  $V(\hat{r}_*)$ . The approximation function is given as

$$R = \sum_i a_i y^i. \quad (20)$$

**Table 1** The coefficients in the approximation function  $R = R(y)$ ,  $\Lambda = 0.1547$ 

$a_0 = 2.366015351$	$a_1 = 0.2008791490 \times 10^{-5}$	$a_2 = 0.6993324845 \times 10^{-11}$
$a_3 = -0.3509900103 \times 10^{-12}$	$a_4 = -0.2066187609 \times 10^{-17}$	$a_5 = 0.7105325819 \times 10^{-19}$
$a_6 = 0.348280473 \times 10^{-24}$	$a_7 = -0.1252082304 \times 10^{-25}$	$a_8 = -0.26504913 \times 10^{-31}$
$a_9 = 0.1676930136 \times 10^{-32}$	$a_{10} = -0.4394063 \times 10^{-39}$	$a_{11} = -0.1580018246 \times 10^{-39}$
$a_{12} = 0.24296543 \times 10^{-45}$	$a_{13} = 0.9980673093 \times 10^{-47}$	$a_{14} = -0.186744938 \times 10^{-52}$
$a_{15} = -0.3999186287 \times 10^{-54}$	$a_{16} = 0.62792831 \times 10^{-60}$	$a_{17} = 0.9157960474 \times 10^{-62}$
$a_{18} = -0.81210131 \times 10^{-68}$	$a_{19} = -0.9109054126 \times 10^{-70}$	

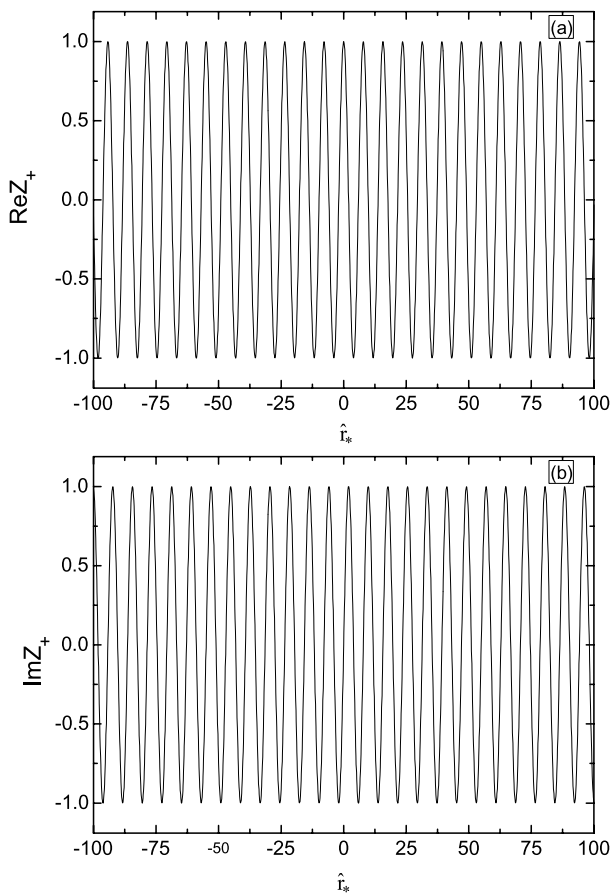
**Fig. 1** The modified tortoise coordinate  $\hat{r}_*$  together with the polynomial approximation  $y$  for  $\Lambda = 0.1547$ **Fig. 2** The potential  $V_+(\hat{r}_*)$  for  $\Lambda = 0.1547$ . This is approximated as a collection of steps

#### 4.1 The Horizons Are Close to Each Other

In this case,  $r_c \rightarrow r_{e+}$ , the coefficient  $\{a_i\}$  is listed in Table 1. Figure 1 shows that the approximation we adopt is of very high accuracy. We take  $R$  and  $r$  as the same, and so do  $y$  and  $\hat{r}_*$ . Then  $V = V(\hat{r}_*)$  is obtained. The variation of  $V_+(\hat{r}_*)$  versus  $\hat{r}_*$  is shown in Fig. 2, it has been replaced by a collection of step functions. In fact, we use as many as 10000 steps to

**Table 2** The coefficients in the approximation function  $R = R(y)$ ,  $\Lambda = 0.001$ 

$a_0 = 2.273858520$	$a_1 = -0.1074981695$	$a_2 = 0.2771754072$
$a_3 = -0.2620447274 \times 10^{-1}$	$a_4 = 0.1669209437 \times 10^{-2}$	$a_5 = -0.7637028850 \times 10^{-4}$
$a_6 = 0.2437721118 \times 10^{-5}$	$a_7 = -0.5273225807 \times 10^{-7}$	$a_8 = 0.7439728299 \times 10^{-9}$
$a_9 = -0.6565383518 \times 10^{-11}$	$a_{10} = 0.3926095206 \times 10^{-13}$	$a_{11} = -0.1896258066 \times 10^{-15}$
$a_{12} = -0.2814022333 \times 10^{-17}$	$a_{13} = 0.9629786026 \times 10^{-19}$	$a_{14} = -0.8422085407 \times 10^{-21}$
$a_{15} = 0.4292410325 \times 10^{-23}$	$a_{16} = -0.9214557213 \times 10^{-25}$	$a_{17} = 0.6606334050 \times 10^{-27}$
$a_{18} = 0.7310061165 \times 10^{-29}$	$a_{19} = -0.6158157973 \times 10^{-31}$	$a_{20} = -0.541607098 \times 10^{-34}$
$a_{21} = -0.3020813079 \times 10^{-35}$	$a_{22} = -0.1534694889 \times 10^{-37}$	$a_{23} = 0.8774520402 \times 10^{-39}$
$a_{24} = -0.4358332655 \times 10^{-41}$		

**Fig. 3** The variation of (a)  $\text{Re}(Z_+)$  and (b)  $\text{Im}(Z_+)$  vs.  $\hat{r}_*$ ,  $\Lambda = 0.1547$ 

accurately follow the shape of the potential so that the steps become indistinguishable from the actual potential function. The wave function on each step is given by quantum mechanics as

$$Z_{+,n} = A_n \exp[i k_n \hat{r}_{*,n}] + B_n \exp[-i k_n \hat{r}_{*,n}], \quad (21)$$

**Fig. 4** The modified tortoise coordinate  $\hat{r}_*$  together with the polynomial approximation  $y$  for  $\Lambda = 0.001$

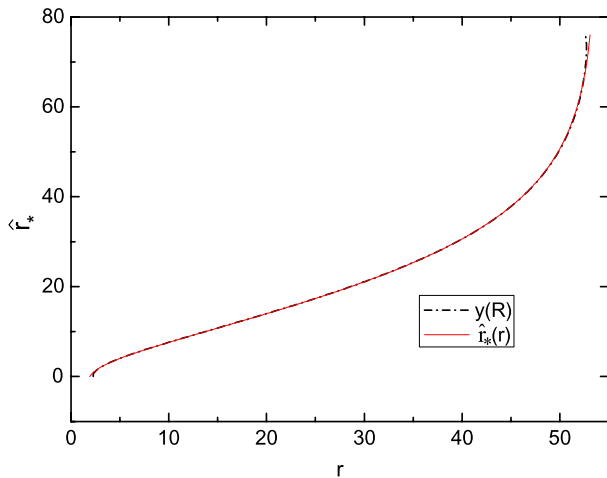
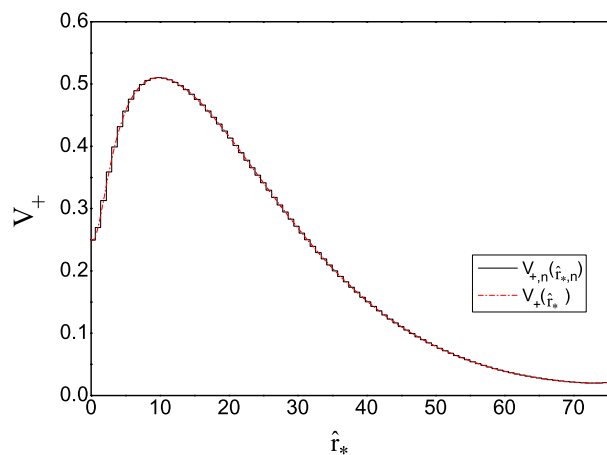


**Fig. 5** The potential  $V_+(\hat{r}_*)$  for  $\Lambda = 0.001$ . This is approximated as a collection of steps



where  $k$  is the wave number ( $k = \sqrt{\sigma^2 - V_+}$ ) and  $k_n$  is its value at the  $n$ th step. The following standard junction conditions are included to ensure the function smooth

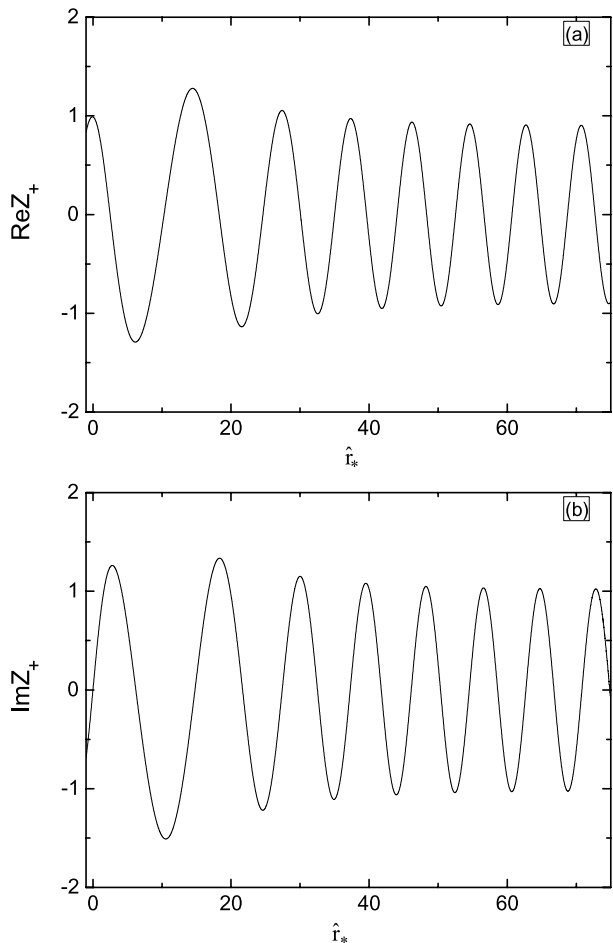
$$Z_{+,n} = Z_{+,n-1}, \quad \left. \frac{dZ_+}{d\hat{r}_*} \right|_n = \left. \frac{dZ_+}{d\hat{r}_*} \right|_{n-1}. \quad (22)$$

Figure 3(a) and (b) show the behavior of the wave function with  $\hat{r}_*$  as the independent coordinate, we can see the amplitudes ( $\text{Re } Z_+$  and  $\text{Im } Z_+$ ) are characteristically similar to the harmonic in the whole range.

#### 4.2 The Horizons Are Widely Separated

In this case,  $r_c \gg r_{e+}$ .  $\{a_i\}$  is listed in Table 2. Figure 4 shows the polynomial approximation and the modified tortoise coordinate together. The approximation is very accurate. Only close to the horizons does the approximation fail. This is because the two horizons are far apart to each other. The variation of the potential in this case is shown in Fig. 5, it is also been

**Fig. 6** The variation of (a)  $\text{Re}(Z_+)$  and (b)  $\text{Im}(Z_+)$  vs.  $\hat{r}_*$ ,  $\Lambda = 0.001$



replaced by a collection of step functions. Figure 6(a) and (b) show how the field amplitudes vary versus  $\hat{r}_*$  within the given region between the horizons. Different from the first case, the amplitude ( $\text{Re}(Z_+)$  or  $\text{Im}(Z_+)$ ) as well as the wavelength has an apparent variation in the whole range.

## 5 Conclusion

In this paper, we solved Dirac equation in RNdS geometry when it is at the phase transition point. When the two horizons are close to each other, the potential is wide but is so low that the waves are almost harmonic in the whole region. When the two horizons are far apart, the potential is narrow and has a peak value as  $\hat{r}_* \rightarrow 13$ . Thus the amplitude is strengthened and the wavelength is prolonged by the potential barrier when the particle transmits toward the black hole. While the waves tend to be harmonic when the particle is far away from the potential barrier. We did not calculate the reflection and transmission coefficients. The reason is that the reflection coefficient always tend to be zero and the transmission coefficient

will be equal to one whatever be the value of the cosmological constant. This result can be concluded by [14, 15, 17].

## References

1. Chandrasekhar, S.: Proc. R. Soc. Lond. A **349**, 571 (1976)
2. Page, D.N.: Phys. Rev. D **14**, 1509 (1976)
3. Khanal, U., Panchapakesan, N.: Phys. Rev. D **24**, 829 (1980)
4. Liu, L., et al.: Acta Phys. Sci. **29**, 1617 (1980)
5. Zhao, Z., et al.: Acta Astrophys. Sin. **1**, 141 (1981)
6. Khanal, U.: Phys. Rev. D **32**, 879 (1984)
7. Chakrabarti, S.K.: Proc. R. Soc. Lond. A **391**, 27 (1984)
8. Semiz, I.: Phys. Rev. D **46**, 5414 (1992)
9. Jin, W.M.: Class. Quantum Gravity **15**, 3163 (1998)
10. Mukhopadhyay, B., Chakrabarti, S.K.: Class. Quantum Gravity **16**, 3165 (1999)
11. Mukhopadhyay, B., Chakrabarti, S.K.: Nucl. Phys. B **582**, 627 (2000)
12. Chakrabarti, S.K., Mukhopadhyay, B.: Nuovo Cimento B **115**, 885 (2000)
13. Chakrabarti, S.K., Mukhopadhyay, B.: Mon. Not. R. Astron. Soc. **317**, 979 (2000)
14. Lyu, Y., Gui, Y.X.: Nuovo Cimento B **119**, 453 (2004)
15. Lyu, Y., Gui, Y.X.: Phys. Scr. **75**, 152 (2007)
16. Lyu, Y., Gui, Y.X.: Int. J. Theor. Phys. **46**, 1596 (2007)
17. Lyu, Y., et al.: Mod. Phys. Lett. A **24**, 2433 (2009)
18. Newman, E., Penrose, R.: J. Math. Phys. **7**, 863 (1966)
19. Goldberg, J.N., et al.: J. Math. Phys. **8**, 2155 (1967)
20. Guo, G.H., et al.: Chin. Phys. Lett. **22**, 820 (2005)